POPULATION OF THE ENTRY STATES IN HEAVY-ION FUSION REACTIONS

D.G. SARANTITES, M. JÄÄSKELÄINEN [1], R. WOODWARD, F.A. DILMANIAN
Department of Chemistry, Washington University, St. Louis, MO 63130, USA

and

D.C. HENSLEY, J.H. BARKER [2], J.R. BEENE, M.L. HALBERT and W.T. MILNER
Oak Ridge National Laboratory, Oak Ridge, TN 37830, USA

Received 8 April 1982

The excitation energy and angular momentum dependence of the population of the entry states following fusion of 136 MeV ^{20}Ne with ^{146}Nd has been measured with a new tpe of instrument. Statistical-model calculations reproduce the main features of the data. Structure effects for $J \gtrsim 45$ are evident in the entry lines. The entrance-channel orbital angular momentum distribution leading to fusion has been deduced.

The study of the dependence on angular momentum and excitation energy of fusion-like reactions and the investigation of the structure of nuclei at high spin and temperature have been a prime focus of experimental heavy-ion physics over the last two decades [1]. The main effects manifest themselves in the population of the entry states, i.e. the states [2,3] in which the residual nuclei are left following the emission of particles. The spin distribution of the entry-state population has been studied by means of γ-ray multiplicity (M_γ) measurements which, in practice, have produced statistically significant information only on the first two moments of the M_γ distribution [4–6]. The excitation-energy distributions have been studied by measurements of particle spectra [7,8]. These experiments gave information only on the projection of the entry-state population on either the spin (J) or excitation energy (E^*) axes. More recently the entry line (average E^* for each J or M_γ of the entry states) has been deduced from measurements using a γ-ray sum spectrometer [9,10].

We report here measurements which provide for the first time detailed information on the entry-state populations for different exit channels as a function of both spin and excitation energy. From these data we are able to infer the entrance channel l-distribution that leads to fusion. The measurements are the first made with the Spin Spectrometer, a new 4π γ-ray detector system consisting of up to 72 NaI counters of equal solid angle [11,12].

A 1.83 mg/cm^2 target of Nd metal enriched to 97.46% in ^{146}Nd was bombarded with a 136.0 MeV ^{20}Ne beam from ORIC. A Ge detector at 117° to the beam provided the triggering signal for the Spin Spectrometer electronics. In this experiment 69 of the 72 NaI detectors in the spectrometer were used, covering 92.3% of 4π. For every trigger, all nonzero pulse heights and associated times relative to the Ge pulse and the Ge time relative to the cyclotron rf were recorded on magnetic tape. A weak ^{88}Y source was placed near the target to monitor gain stability during data acquisition.

The event tapes were first processed to (1) correct for nonlinearities in the NaI pulse-height response, (2) match the gains of all the NaI elements, (3) correct for pulse-height dependence of the timing, (4) derive an accurate reference time for each event by averaging

[1] On leave from Department of Physics, University of Jyväskylä, Jyväskylä, Finland.

[2] Oak Ridge Associated Universities Research Participant: on leave from St. Louis University, St. Louis, MO 63103, USA. Present address: South Carolina Electric & Gas Company, Columbia, SC 29218, USA.

0 031-9163/82/0000–0000/$02.75

the times of the NaI γ-ray pulses, and (5) separate neutron and γ-ray pulses by their time of flight. Neutron rejection of better than 95% for pulse heights $h_i > 80$ keV was accomplished by setting an appropriate mask on the (h_i, t_i) map for each detector. The processed events were then sorted to construct a Ge spectrum for each coincidence fold (k) and each 1.0 MeV interval in total pulse height (H). The areas of the Ge peaks due to the $2^+ \rightarrow 0^+$ or $17/2^+ \rightarrow 13/2^+$ yrast transitions in $^{158-161}$Yb (xn channels) and $^{155-158}$Er (αxn channels) were determined by least-squares fits with gaussian peak shapes to provide the population distribution, $Q_x(H, k)$, for each exit channel x. As an example, fig. 1a shows a density plot of $Q_{6n}(H, k)$.

The populations $R_x(E^*, M_\gamma)$ for excitation energy E^* and multiplicity M_γ were then obtained by solving the system of equations

$$\sum_{E^*, M_\gamma} P(E^*, M_\gamma \rightarrow H, k)\, R_x(E^*, M_\gamma) = Q_x(H, k)\,. \tag{1}$$

by an iterative least-squares procedure. The response functions of the spectrometer, $P(E^*, M_\gamma \rightarrow H, k)$, for M_γ = 1 to 60 and E^* = 1 to 60 MeV were constructed from data taken with ^{111}In, ^{207}Bi, ^{152}Eu, ^{60}Co, ^{88}Y, and ^{24}Na sources. The properties of $P(E^*, M_\gamma \rightarrow H, k)$ are discussed in refs. [11] and [12], and the experimental calibration procedures have been described in ref. [13]. The responses used in the present analysis were initially constructed by assuming M_γ equal-energy γ rays with $E_\gamma = E^*/M_\gamma$. These responses have been compared with those from a more realistic E_γ spectrum. The equal-energy assumption correctly reproduces the average response properties and the projected k response, but it underestimates the width of the response along the H coordinate for a given (E^*, M_γ). Corrections for this effect were applied to the responses used in the final analysis. Small corrections for angular-correlation effects based on Monte Carlo simulations were applied to the $R_x(E^*, M_\gamma)$ populations. Corrections to E^* and M_γ for the gating transition and to M_γ for internal conversion were also made.

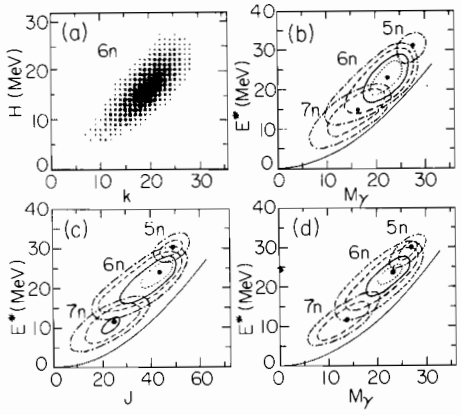

Fig. 1. Entry-state distributions for xn products from 136 MeV ^{20}Ne on ^{146}Nd. (a) Experimental density map in (H, k) space for the 6n channel. (b) Contour maps of experimental results in (E^*, M_γ) space for the strongest xn channels. (c) Contour maps of calculated results in (E^*, J) space from the statistical model. (d) Contour map of results in (E^*, M_γ) space from the same calculations as in (c). The cross-section contours in (b), (c) and (d) decrease going outward by the factors of 1.4, 2.0, 4.0 and 8.0 relative to the peak value of the 6n channel and are represented by the dotted, full, dashed and dashed–dotted curves, respectively. The heavy dots locate the maximum intensity for each channel. The ^{160}Yb yrast line used in the calculations is shown by the curve below the contours.

Entry-state populations in (E^*, M_γ) space for the various xn exit channels are shown in fig. 1b. The projections of the entry-state populations on the M_γ and E^* axes are shown (data points) in figs. 2a and 2b, respectively. Some of the angular momentum in the odd-A channels is removed by low energy or delayed transitions that were not detected by the spectrometer. The M_γ distributions for these channels have been shifted by 2.2 units to compensate for these undetected transitions.

Statistical-model calculations were carried out using the Monte Carlo code JULIAN–PACE [14] modified for a more realistic treatment of γ-ray strengths. The initial l distributions were assumed to be of the form $(2l + 1)\{1 + \exp[(l - l_{fus})/d]\}^{-1}$. Reasonable agreement with experiment was obtained with l_{fus} = 59.5 and d = 1 (σ_{fus} = 1138 mb). This distribution is a close approximation to that predicted by the sum rule model [15]; the Bass model [16] gives l_{fus} = 62.6 (σ_{fus} = 1278 mb). Fig. 2f shows initial l distributions for two values of the diffuseness (d = 1 and 5) and l_{fus} = 59.5, and the resulting total entry-state J distributions for the evaporation residues from the $xn + \alpha xn$ channels. The level-density parameter was $a = A/9.5$. The E1 γ-ray emission strength function included the giant dipole resonance [17–19] with shape and position taken from experimental systematics [20,21] and strength determined by the energy weighted sum rule [21]. Statistical E2 and M1 transitions were included with B(E2) = 1.0 WU and B(M1) = 0.005 WU, together with col-

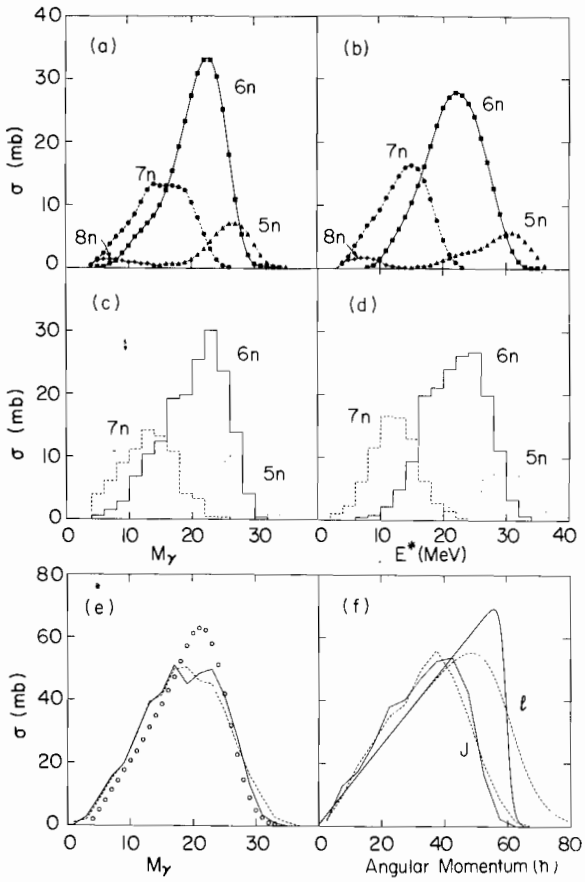

Fig. 2. Projections of entry-state distributions. (a) Experimental cross sections of the xn channels as a function of M_γ. (b) Experimental cross sections of the xn channels as a function of E^*. (c) Calculated cross sections of the xn channels as a function of M_γ. (d) Calculated cross sections of the xn channels as a function of E^*. The calculations are based on an entrance-channel l distribution with $l_{fus} = 59.5$ and a diffuseness $d = 1$. (e) Experimental cross sections (points) and calculated J distributions (lines) for the sum of the xn and αxn channels as a function of M_γ. (f) Calculated entrance-channel l distributions and the resulting J distributions summed over all xn and αxn channels. The calculated results in (e) and (f) are for $d = 1$ (solid lines) and $d = 5$ (dashed lines).

lective stretched E2 transitions with $B(E2) = 100$ WU for $E_\gamma \leqslant 2.0$ MeV. With these parameters the Monte Carlo γ cascades proceeded to the vicinity of the yrast line and then were assumed to reach the ground state or an yrast state with $J < 2$ by stretched E2 transitions [14]. The yrast lines were taken from the rotating liquid drop model [22] above spin 22; below $J = 22$ the moment of inertia was assumed to decrease linearly with decreasing J to approximate the behavior typical of rotational nuclei. The calculated entry populations in (E^*, J) and in (E^*, M_γ) space are shown in figs. 1c and 1d, respectively, for the xn exit channels.

Projections on the M_γ and E^* axes of the calculated entry state populations for the xn channels are shown in figs. 2c and 2d. The agreement with experiment is reasonably good. Part of the discrepancy between the M_γ projections for the 7n channel could arise from an overcorrection for the undetected transitions due to lack of knowledge of the decay scheme for ^{159}Yb.

The calculations appear to provide a direct connection between the initial l distribution and the total J distribution. Variations in the level density and E1 strength which preserve the agreement with the experimental M_γ and E^* projections for the various exit channels do not affect the relationship between the l and J distributions significantly. Fig. 2e shows a comparison between the experimental data (points) and calculations (histograms) using $d = 1$ and 5 for the sum over xn and αxn channels. Large values of d underestimate both the slope of the upper edge and the most probable value of M_γ. We conclude that a rather small diffuseness ($d < 2$) is required. The pxn channels and channels involving multiple charged-particle evaporation were not analyzed. These are predicted by the theory to account for ~20% of the fusion cross section, but the calculations show that our conclusions on the entrance-channel l distribution are not sensitive to the omission of these channels.

The experimental and calculated entry lines for the

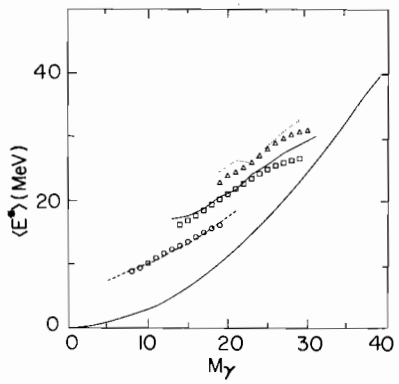

Fig. 3. Entry lines for the principal xn channels. The points represent experimental results (△ = 5n, □ = 6n, ○ = 7n) while the lines are the results of statistical-model calculations. The lowest curve is the yrast line used in the calculations.

xn channels are compared in fig. 3. Good agreement is observed for the positions and the slopes for the main part of the entry lines. However, the experimental data show a significant decrease in slope for ^{161}Yb and ^{160}Yb at $M_\gamma \sim 28$ and 26, respectively. This effect cannot be reproduced by the statistical model with any reasonable variation of the parameters that does not involve a significant decrease in the slope of the yrast line or a drastic change in the decay mode of the entry states for $J \gtrsim 45$ (e.g. an increased number of $\Delta J = 1$ transitions). Either of these possibilities would suggest a dramatic change in nuclear structure over a narrow spin range. The origin of this effect needs further investigation.

The experimental and theoretical (E^*, M_γ) distributions are shown in figs. 1b and 1d. Although the calculated projections on the E^* and M_γ axes and the entry lines generally agree with the data, the two-parameter distributions are noticeably different; the calculated ones are about 30% narrower in the direction perpendicular to the entry line. This discrepancy is essentially independent of the level-density parameter (from $a = A/7.5$ to $A/10.5$) and the E1 strength (from 1.0 to 1.8 times the energy weighted sum rule). It may be a consequence of the simplified treatment of the level densities and the γ-decay properties in these calculations.

In summary, we have measured the population of entry states over a large range of excitation energies and spins. Statistical-model calculations in which the entrance-channel l distribution is chosen to have a sharp upper edge reproduce the data quite well except for the widths of the two-parameter distributions. However, a significant change in the slope of the entry lines at high spin values is found that cannot be explained by reasonable statistical-model parameters. This seems to imply either a change in slope of the yrast line or a change of the decay mode of the entry states for $J \gtrsim 45$.

This work was supported in part by the US Department of Energy under contract no. DE-A502-76ER-4052. Oak Ridge National Laboratory is operated by Union Carbide Corporation for the US Department of Energy under contract no. W-7405-eng-26.

References

[1] R.M. Diamond and F.S. Stephens, Ann. Rev. Nucl. Part. Sci. 30 (1980) 85.
[2] J.R. Grover and J. Gilat, Phys. Rev. 157 (1967) 802, 814.
[3] D.G. Sarantites and B.D. Pate, Nucl. Phys. A93 (1966) 545.
[4] P.O. Tjøm et al., Phys. Rev. Lett. 33 (1974) 593.
[5] G.B. Hagemann et al., Nucl. Phys. A245 (1975) 166.
[6] D.G. Sarantites et al., Phys. Rev. C14 (1976) 2138.
[7] D.G. Sarantites and E.J. Hoffman, Nucl. Phys. A180 (1972) 177.
[8] J.J. Simpson et al., Nucl. Phys. A287 (1977) 362.
[9] P.O. Tjøm et al., Phys. Lett. 72B (1978) 439.
[10] F. Folkmann et al., Nucl. Phys. A361 (1981) 242.
[11] D.G. Sarantites et al., Nucl. Instrum. Methods 171 (1980) 503.
[12] D.G. Sarantites et al., J. Phys. (Paris) Coll. C10, 41 (1980) 269.
[13] M. Jääskeläinen et al., submitted for publication in Nucl. Instrum. Methods.
[14] M. Hillman and Y. Eyal, Code JULIAN, unpublished; A. Gavron, modification PACE, Phys. Rev. C21 (1980) 230.
[15] J. Wilczynski et al., Phys. Rev. Lett. 45 (1980) 606.
[16] R. Bass, Phys. Rev. Lett. 39 (1977) 265.
[17] J.H. Barker and D.G. Sarantites, Phys. Rev. C9 (1974) 607.
[18] J.O. Newton et al., Phys. Rev. Lett. 46 (1981) 1383.
[19] G.A. Bartholomew et al., Advances in nuclear physics, eds. M. Baranger and E. Vogt, Vol. 7 (1973) p. 229.
[20] S.S. Hanna, in: Giant multipole resonances, ed. F. Bertrand (Harwood, New York, 1980) Table I.
[21] A. Bohr and B.R. Mottelson, Nuclear structure, Vol. II (Benjamin, Reading, MA, 1975) 474ff.
[22] S. Cohen, F. Plasil and W.J. Swiatecki, Ann. Phys. (NY) 82 (1974) 557.